Pancreatic Endoplasmic Reticulum Kinase Activation Promotes Medulloblastoma Cell Migration and Invasion through Induction of Vascular Endothelial Growth Factor A

Stephanie Jamison[1,2,3], Yifeng Lin[1,2,3¤], Wensheng Lin[1,2,3]*

1 Department of Neuroscience, University of Minnesota, Minneapolis, United States of America, 2 Institute for Translational Neuroscience, University of Minnesota, Minneapolis, United States of America, 3 Masonic Cancer Center, University of Minnesota, Minneapolis, United States of America

¤ Current address: Institute of Pediatrics, Children's Hospital, Fudan University, Shanghai, China
* linw@umn.edu

Abstract

Evidence is accumulating that activation of the pancreatic endoplasmic reticulum kinase (PERK) in response to endoplasmic reticulum (ER) stress adapts tumor cells to the tumor microenvironment and enhances tumor angiogenesis by inducing vascular endothelial growth factor A (VEGF-A). Recent studies suggest that VEGF-A can act directly on certain tumor cell types in an autocrine manner, via binding to VEGF receptor 2 (VEGFR2), to promote tumor cell migration and invasion. Although several reports show that PERK activation increases VEGF-A expression in medulloblastoma, the most common solid malignancy of childhood, the role that either PERK or VEGF-A plays in medulloblastoma remains elusive. In this study, we mimicked the moderate enhancement of PERK activity observed in tumor patients using a genetic approach and a pharmacologic approach, and found that moderate activation of PERK signaling facilitated medulloblastoma cell migration and invasion and increased the production of VEGF-A. Moreover, using the VEGFR2 inhibitor SU5416 and the VEGF-A neutralizing antibody to block VEGF-A/VEGFR2 signaling, our results suggested that tumor cell-derived VEGF-A promoted medulloblastoma cell migration and invasion through VEGFR2 signaling, and that both VEGF-A and VEGFR2 were required for the promoting effects of PERK activation on medulloblastoma cell migration and invasion. Thus, these findings suggest that moderate PERK activation promotes medulloblastoma cell migration and invasion through enhancement of VEGF-A/VEGFR2 signaling.

Introduction

The unfolded protein response (UPR), activated by endoplasmic reticulum (ER) stress, coordinates an adaptive program to preserve cell function and survival under stressful conditions [1, 2]. The UPR is mediated by three ER-resident transmembrane proteins, pancreatic ER kinase

(PERK), inositol requiring enzyme 1 (IRE1), and activating transcription factor 6 (ATF6). PERK activation inhibits global protein biosynthesis, but stimulates the expression of certain stress-induced cytoprotective genes by phosphorylating translation initiation factor 2α (eIF2α) [3]. Phosphorylation of eIF2α enhances the expression of growth arrest and DNA damage 34 (GADD34), a regulatory subunit of a phosphatase complex that dephosphorylates eIF2α, by promoting the translation of the cytosolic transcription factor ATF4, which forms a negative feedback to down-regulate PERK signaling [4]. It has been well documented that the UPR is activated in solid tumors due to hypoxia and nutritional deficiency, a common feature of the solid tumor microenvironment [5–7]. Nevertheless, the role of the PERK branch of the UPR in tumor development is controversial [8, 9]. Some studies show that PERK activation facilitates tumor development by promoting tumor cell survival and enhancing angiogenesis [10–12]. Other studies show that PERK activation inhibits tumor cell proliferation and leads to cell apoptosis [13–15].

Medulloblastoma is the most common solid malignancy of childhood [16, 17]. Our previous study showed that the UPR is activated in tumor cells in a mouse model of medulloblastoma and that GADD34 inactivation enhances PERK signaling and facilitates the medulloblastoma formation by promoting angiogenesis through induction of vascular endothelial growth factor A (VEGF-A) [18]. It is known that tumor cell-derived VEGF-A acts on endothelial cells to promote angiogenesis and tumor progression [19]. Recent studies also suggest that VEGF-A can act directly on some types of tumor cells in an autocrine manner, via binding to VEGF receptor 2 (VEGFR2), to promote tumor cell growth, migration, and invasion [20, 21]. Intriguingly, a previous report suggests a possible autocrine role of VEGF-A in human medulloblastoma growth [22]. Moreover, several studies show that PERK activation in human medulloblastoma cells enhances the expression of VEGF-A [23, 24]. Thus, we hypothesized that PERK activation promotes medulloblastoma cell migration and invasion by enhancing autocrine VEGF-A/VEGFR2 signaling.

To test this hypothesis experimentally, we first generated stably transfected medulloblastoma cell lines that allow for pharmacologically controlled activation of PERK without causing ER stress. We used the cell lines to mimic the enhancement of PERK activity to levels observed in tumor patients and determined its effects on tumor cells, thus enabling a critical evaluation of the role of PERK signaling in medulloblastoma cell migration and invasion. Our findings uncover the promoting role of PERK signaling in medulloblastoma cell migration and invasion and its underlying mechanism.

Materials and Methods

Cell culture

The Daoy cells were purchased from American Type Culture Collection (item number HTB-186, Manassas, VA). The UW228 cells [25] were a generous gift from Dr. John Silber (University of Washington, Seattle, WA). Both Daoy and UW228 cells were maintained in Dulbecco's Modified Eagle Medium (DMEM; Invitrogen, Carlsbad, CA) supplemented with 10% Fetal Bovine Serum (FBS, Invitrogen) and 1% penicillin/streptomycin (Invitrogen) at 37°C with 5% CO_2. The Fv2E-PERK cDNA clone was a generous gift from Dr. David Ron (Cambridge University, Cambridge, UK). A 2.4 kb Fv2E-PERK cDNA segment was excised from the pBabe/Fv2E-PERK plasmid [26] with EcoRI and ApaI and was inserted into the multiple cloning sites region of the pcDNA3.1 plasmid (Invitrogen) at the same restriction sites. The resulting pcDNA3.1-Fv2E-PERK was further digested with EcoRI and PmeI to release the Fv2E-PERK cDNA, which was subcloned into the multiple cloning sites region of the pIREs-ZsGreen (Clontech Laboratories, Inc., Mountain View, CA) at the EcoRI and SmaI sites. Daoy cells were

transfected with the mammalian expression plasmid pIREs-Fv2E-PERK-ZsGreen that contains the neomycin resistance gene using Lipofectamine 2000 transfection reagent (Invitrogen) according to the manufacturer's instructions. The stably transfected cell lines were selected with 500 µg/ml G418 (Invitrogen).

Western blot analysis

Near-confluent cells were treated with either AP20187 (Clontech Laboratories, Inc.), Salubrinal (EMD Millipore, Billerica, MA), GSK2606414 (EMD Millipore), or vehicle (either ethanol or DMSO) for 2 h. Cells were rinsed with ice-cold PBS and were immediately homogenized in 5 volume of Triton X-100 buffer as previously described [27, 28]. After incubating on ice for 10 min, the extracts were cleared by centrifugation at 14,000 rpm for 20 min. The protein content of each extract was determined by DC Protein Assay (Bio-Rad Laboratories, Hercules, CA). The extracts (20 µg) were separated by SDS-PAGE and were transferred to nitrocellulose. The blots were incubated with primary antibody (see below), and the signal was revealed by chemiluminescence after reacting with HRP-conjugated secondary antibody. The following primary antibodies were used: anti-FKBP-12 (polyclonal, anti-rabbit, cat# PA1–026A, 1:2000, Thermo Scientific, Rockford, IL); eIF2α (polyclonal, anti-rabbit, cat# SC-11386, 1:1000, Santa Cruz Biotechnology, Dallas, TX); phosphorylated eIF2α (p-eIF2α, anti-rabbit, cat# 9721L, 1:1000; Cell Signaling Technology, Beverly, MA), and actin (anti-rabbit, cat# A2103, 1:5000; Sigma-Aldrich, St. Louis, MO). The intensity of the recorded chemiluminescence signal was quantified using NIH ImageJ software (http://rsb. info.nih.gov/ij).

MTT assay

Cells were plated 1×10^4 per well in 96-well microtiter plates and incubated in DMEM with 10% FBS for 24 h. Then, either AP20187, SU5416 (Sigma-Aldrich), VEGF-A neutralizing antibody (NAB, R&D Systems, Minneapolis, MN), or vehicle (either ethanol, DMSO, or PBS with control mouse IgG) was added to the media and the cultures were incubated for additional 16 h. Cell viability was determined by the MTT Assay Kit (Promega, Madison, WI) according to the manufacturer's instructions.

Real-time PCR

Near-confluent cells were treated with either AP20187, Salubrinal, or vehicle (either ethanol or DMSO) for 16 h, and then were rinsed with ice-cold PBS. RNA was isolated from cells using TRIzol reagent (Invitrogen) and was treated with DNaseI (Invitrogen) to eliminate genomic DNA. Reverse transcription was performed using the iScript cDNA Synthesis Kit (Bio-Rad Laboratories). Real-time PCR was performed with iQ Supermix (Bio-Rad Laboratories) on the LightCycler 480 System (Roche Diagnostics Corporation, Indianapolis, IN) as previously described [29–32].

Measurement of protein synthesis with surface sensing of translation (SUnSET)

We used SUnSET to determine the rate of protein biosynthesis in cells [31, 33]. Near-confluent cells were treated with AP20187 or vehicle (ethanol). After 1 h, 1 µM puromycin (Sigma-Aldrich) was added to the cultures, and the cultures were incubated for an additional 1 h. Proteins were extracted, quantified, resolved by SDS-PAGE, and transferred to nitrocellulose. The blots were incubated with a primary antibody against puromycin (monoclonal, anti-mouse, cat# MABE343, 1:5000, EMD Millipore), followed by an HRP-conjugated secondary antibody,

and following incubation with the ECL Detection Reagents (GE Healthcare Biosciences, Piscataway, NJ), the chemiluminescent signal was detected.

Wound healing assay

Cells were cultured to confluence in 12-well plates. The confluent monolayers were scratched with a sterile 200 µl pipet tip. The cells were raised with PBS, and then incubated in DMEM with 0.5% FBS and various treatments. Images were taken by phase contrast microscopy using the 10 × objective at the beginning (0 h) and after 16 h of incubation. The wound areas were quantified at 0 h and after 16 h of incubation using NIH Image J program (http://imagej.nih.gov/ij/). The percentage of filled wound area was calculated as the filled wound area at 16 h (the wound area at 0 h—the wound area at 16 h) divided by the wound area at 0 h.

Matrigel transwell assay

The cell culture chambers (8 µm pore membranes, BD Biosciences, Bedford, MA) inserted in a 24-well plate were coated with matrigel (300 µg/ml, BD Biosciences). $0.1–1 \times 10^5$ cells were plated in the top well of a matrigel-coated chamber. Both the top well and the lower well of the chamber were filled with DMEM with 0.5% FBS and various treatments. After 16 h of incubation, non-invading cells were removed with a cotton swab and the invading cells that had crossed the matrigel to the underside of the membrane were stained with crystal violet and photographed. The stained cells were dissolved in 10% acetic acid and the absorbance was measured at 561 nm.

Enzyme-linked immunosorbent assay (ELISA)

Cells were plated 1×10^5 per well in 12-well plates. After 24 h, the cells were raised with PBS, and then incubated in DMEM with 0.5% FBS and various treatments for 16 h. We quantified VEGF-A in the culture supernatants of the wells using human VEGF-A ELISA kit (Thermo Scientific) according to the manufacturer's instructions.

Statistics

Data are expressed as mean ± standard deviation (SD). Multiple comparisons were statistically evaluated by a 1-way ANOVA test using Sigmaplot 12 software (Systat Software, Inc., Chicago, IL). P values less than 0.05 were considered significant.

Results

Moderate PERK activation promotes medulloblastoma cell migration and invasion

The three functional domains of PERK are: a stress-sensing ER luminal domain, an ER transmembrane domain, and a cytosolic eIF2α kinase domain [34]. During ER stress, the stress-sensing ER lumenal domain senses the stress signal and initiates PERK oligomerization and autophosphorylation, resulting in activation of PERK signaling. Fv2E-PERK, an artificial PERK derivative, is generated by fusing the eIF2α kinase effector domain of PERK to a polypeptide containing tandem modified FK506 binding domains (Fv2E). It has been demonstrated that Fv2E-PERK can be induced to oligomerize and activate by an otherwise inert ligand, AP20187, in the absence of any additional stress [26]. We transfected human medulloblastoma cell line Daoy with plasmid pIREs-Fv2E-PERK-ZsGreen and obtained several stably transfected cell lines that were resistant to G418 and expressed various levels of Fv2E-PERK (Fig. 1A). The effects of overexpression of Fv2E-PERK alone on Daoy cell growth, migration,
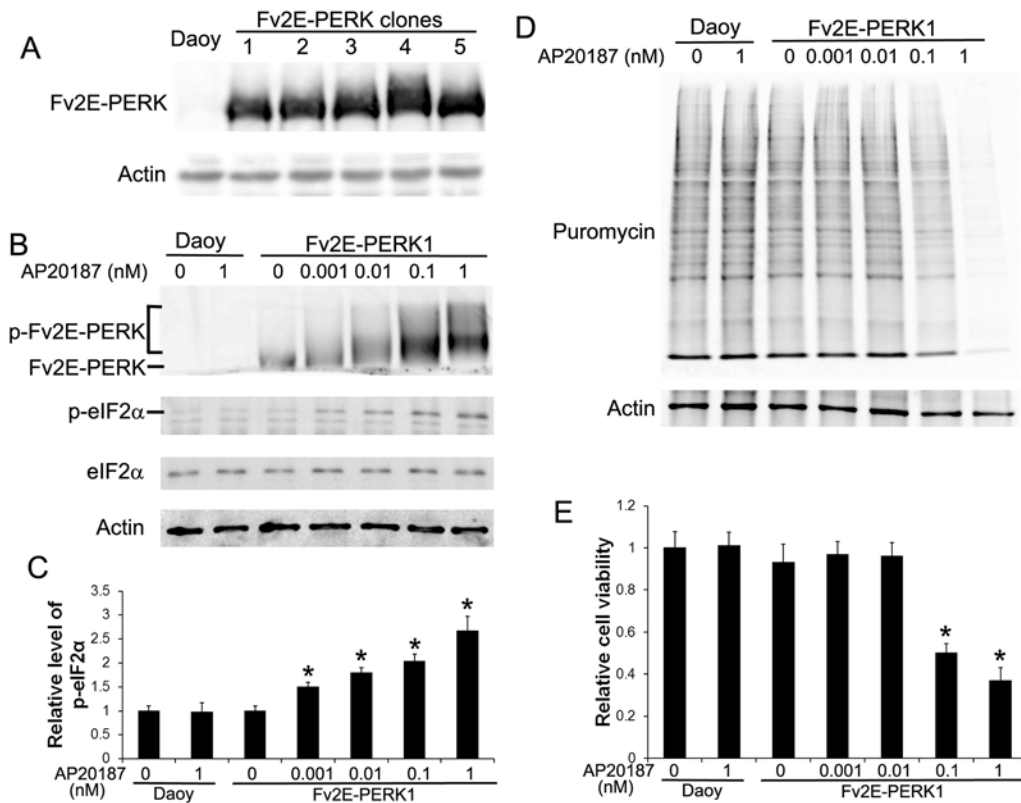
Fig 1. Characterization of stably transfected Daoy cell lines that allow for pharmacological controlled activation of PERK. (A) Daoy cells were transfected with the plasmid pIREs-Fv2E-PERK-ZsGreen. We obtained several stably transfected cell lines that were resistant to G418 and expressed various levels of Fv2E-PERK. (B) Western blot analysis showed that AP20187 treatment activated Fv2E-PERK and led to phosphorylation of eIF2α. The positions of activated Fv2E-PERK (p-Fv2E-PERK) and inactive Fv2E-PERK proteins were indicated. (C) Densitometry analysis of western blot results showed that AP20187 treatment increased the level of p-eIF2a in Fv2E-PERK1 cells in a dose-dependent manner. The relative protein levels are relative to actin. (D) SUnSET measurement of protein biosynthesis revealed dramatic reduction of protein biosynthesis in Fv2E-PERK1 cells treated with the high dose of AP20187 (0.1–1 nM). Nevertheless, treatment with the low dose of AP20187 (0.001–0.01 nM) only slightly reduced protein biosynthesis in the cells. (E) MTT analysis showed that treatment with the high dose of AP20187 (0. 1–1 nM) significantly inhibited Fv2E-PERK1 cell growth. Nevertheless, treatment with the low dose of AP20187 (0.001–0.01 nM) had no effect on the cell growth. The experiments were repeated at least three times. Error bars represent SD, *$P < 0.05$.

doi:10.1371/journal.pone.0120252.g001

and invasion were determined. We found that stably transfected Daoy cell line # 1 (Fv2E-PERK1) expressed a high level of Fv2E-PERK and that overexpression of Fv2E-PERK alone did not significantly affect the cell growth, migration, and invasion as compared to control Daoy cells (Figs. 1, 2). Thus, Fv2E-PERK1 cell line was selected for all subsequent studies.

Importantly, we found that treatment with Fv2E ligand AP20187 had no effect on control Daoy cells (Figs. 1, 2), but triggered the transgenic product Fv2E-PERK activation in Fv2E-PERK1 cells in a dose-dependent manner. Western blot analysis using the anti-FKBP-12 antibody, which recognizes the modified FK506 binding domain and has been successfully used to detect both the unphosphorylated and phosphorylated forms of Fv2E-PERK [8, 29], showed that treatment with AP20187 (0.001–1 nM) triggered phosphorylation of Fv2E-PERK in Fv2E-PERK1 cells in a dose-dependent manner (Fig. 1B). PERK activation inhibits global protein translation by phosphorylating eIF2α. Western blot analysis for p-eIF2α also showed that AP20187 (0.001–1 nM) treatment elevated the level of p-eIF2α in the cells in a dose-dependent manner (Fig. 1B, C). Moreover, we assessed the activity of the PERK-eIF2α pathway in Fv2E-PERK1 cells by measuring the rate of protein biosynthesis using SUnSET, a puromycin-based technology. Interestingly, we found that treatment with the high dose of AP20187 (0.1–1 nM)
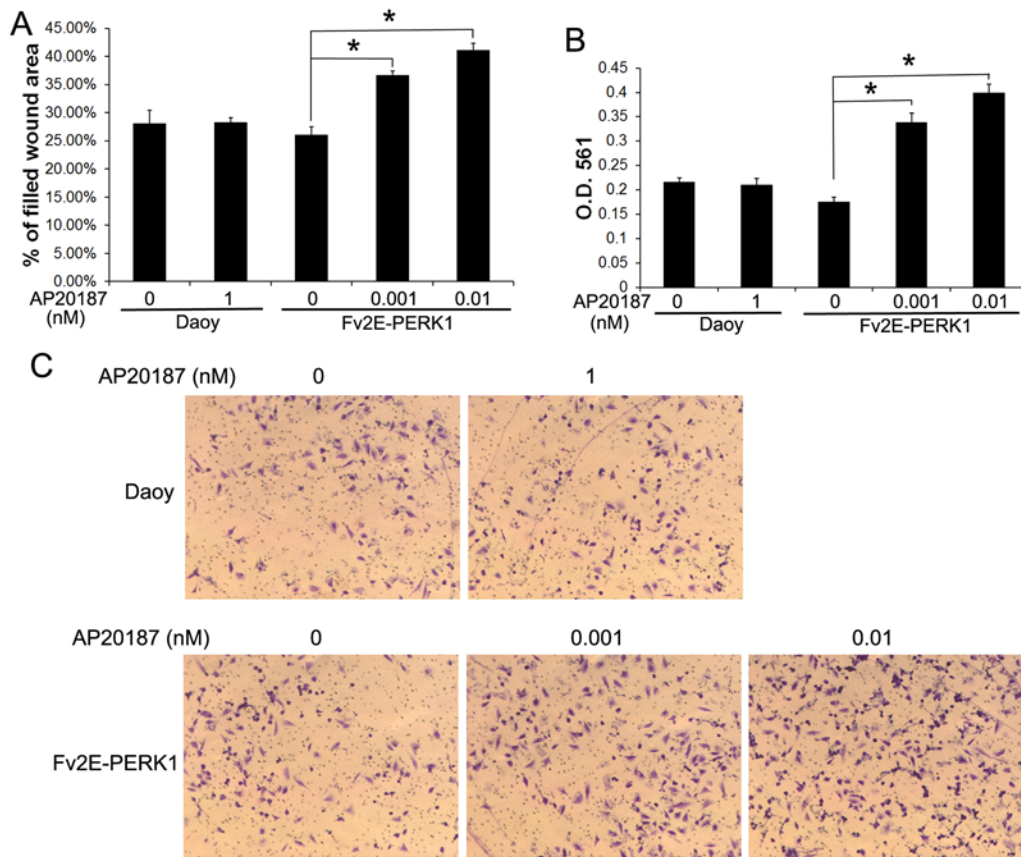
Fig 2. Moderate PERK activation promoted Daoy cell migration and invasion. (A) Wound healing assay showed that AP20187 (0.001–0.01 nM) treatment significantly increased the percentage of filled wound area of Fv2E-PERK1 cells. (B, C) Results of matrigel transwell assay. Daoy or Fv2E-PERK1 cells were seeded in the top well of a matrigel-coated chamber. After 16 h, the invaded cells at the lower surface of the chamber were stained with crystal violet and photographed (C). The stained cells were dissolved in 10% acetic acid and the absorbance was measured at 561 nm (B). AP20187 (0.001–0.01 nM) treatment significantly increased the invaded Fv2E-PERK1 cell numbers at the lower surface of the chamber. The experiments were repeated at least three times. Error bars represent SD, $*P < 0.05$.

doi:10.1371/journal.pone.0120252.g002

dramatically reduced protein biosynthesis in Fv2E-PERK1 cells; however, treatment with the low dose of AP20187 (0.001–0.01 nM) only slightly reduced protein biosynthesis (Fig. 1D). As expected, real-time PCR analysis showed that AP20187 treatment increased the expression of PERK responsible genes CAATT enhancer binding protein homologous protein (CHOP) and GADD34, but did not significantly affect the expression of binding immunoglobulin protein (BIP) (Fig. 3A). Previous reports have shown that induction of CHOP and GADD34 was completely dependent on the activity of PERK during ER stress and the effect of PERK signaling on BIP induction was minimal [29–31, 35]. Therefore, these data suggest that AP20187 treatment exclusively enhances the activity of PERK in Fv2E-PERK1 cells without affecting the other branches of the UPR. Additionally, MTT assay showed that the growth of Fv2E-PERK1 cells was significantly inhibited by the high dose of AP20187 (0.1–1 nM) treatment, but not by the low dose of AP20187 (0.001–0.01 nM) treatment (Fig. 1E). Taken together, these results suggest that the high dose of AP20187 treatment strongly activates PERK signaling in Fv2E-PERK1 cells and inhibits cell growth. Nevertheless, the low dose of AP20187 treatment moderately activates PERK signaling in Fv2E-PERK1 cells, but does not affect cell growth. It is generally believed that ER stress and the UPR activation under physiological and pathological conditions are moderate [31, 36]. Thus, to mimic the moderate PERK activation under
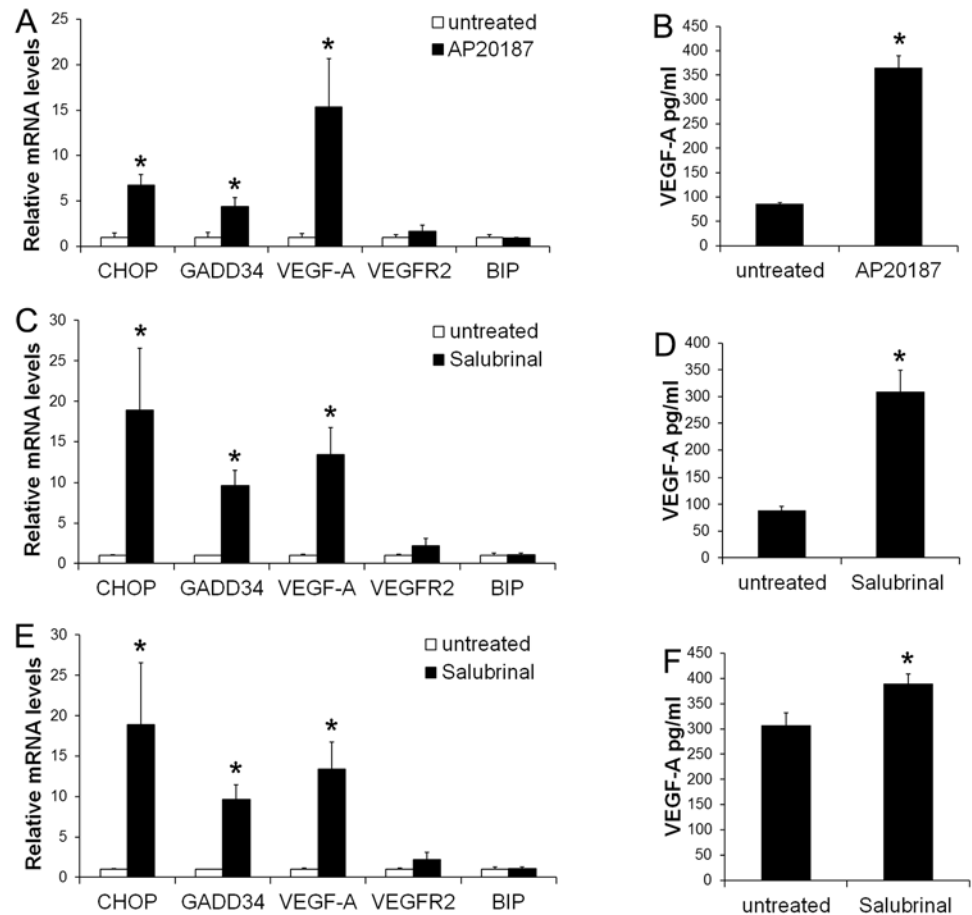
Fig 3. PERK activation stimulated medulloblastoma cells to produce VEGF-A. (A) Real-time PCR analysis showed that 0.01 nM AP20187 treatment significantly increased the expression of CHOP, GADD34, and VEGF-A in Fv2E-PERK1 cells, but did not affect the expression of VEGFR2 and BIP. (B) ELISA analysis showed that 0.01 nM AP20187 treatment significantly increased the production of VEGF-A in Fv2E-PERK1 cells. (C) Real-time PCR analysis showed that 10 μM Salubrinal treatment significantly increased the expression of CHOP, GADD34, and VEGF-A in Daoy cells, but did not affect the expression of VEGFR2 and BIP. (D) ELISA analysis showed that 10 μM Salubrinal treatment significantly increased the production of VEGF-A in Daoy cells. (E) Real-time PCR analysis showed that 10 μM Salubrinal treatment significantly increased the expression of CHOP, GADD34, and VEGF-A in UW228 cells, but did not affect the expression of VEGFR2 and BIP. (F) ELISA analysis showed that 10 μM Salubrinal treatment significantly increased the production of VEGF-A in UW228 cells. The experiments were repeated at least three times. Error bars represent SD, $*P < 0.05$.

doi:10.1371/journal.pone.0120252.g003

pathological conditions, Fv2E-PERK1 cells were treated with the low dose of AP20187 (0.01 nM) for all subsequent studies.

Next, we determined the effects of moderate PERK activation on medulloblastoma cell migration and invasion. Wound healing assay showed that treatment with the low dose of AP20187 (0.001–0.01 nM) significantly increased the migration capacity of Fv2E-PERK1 cells into the wounds (Fig. 2A). Matrigel transwell assay showed that the low dose of AP20187 (0.001–0.01 nM) treatment significantly enhanced the capacity of Fv2E-PERK1 cells to invade through the matrigel (Fig. 2B, C). Finally, we verified the effects of moderate PERK activation on medulloblastoma cell migration and invasion using a pharmacologic approach. Medulloblastoma cell lines, Daoy and UW228, were treated with either Salubrinal, a small chemical compound that inhibits the activity of the phosphatase complex that dephosphorylates eIF2α

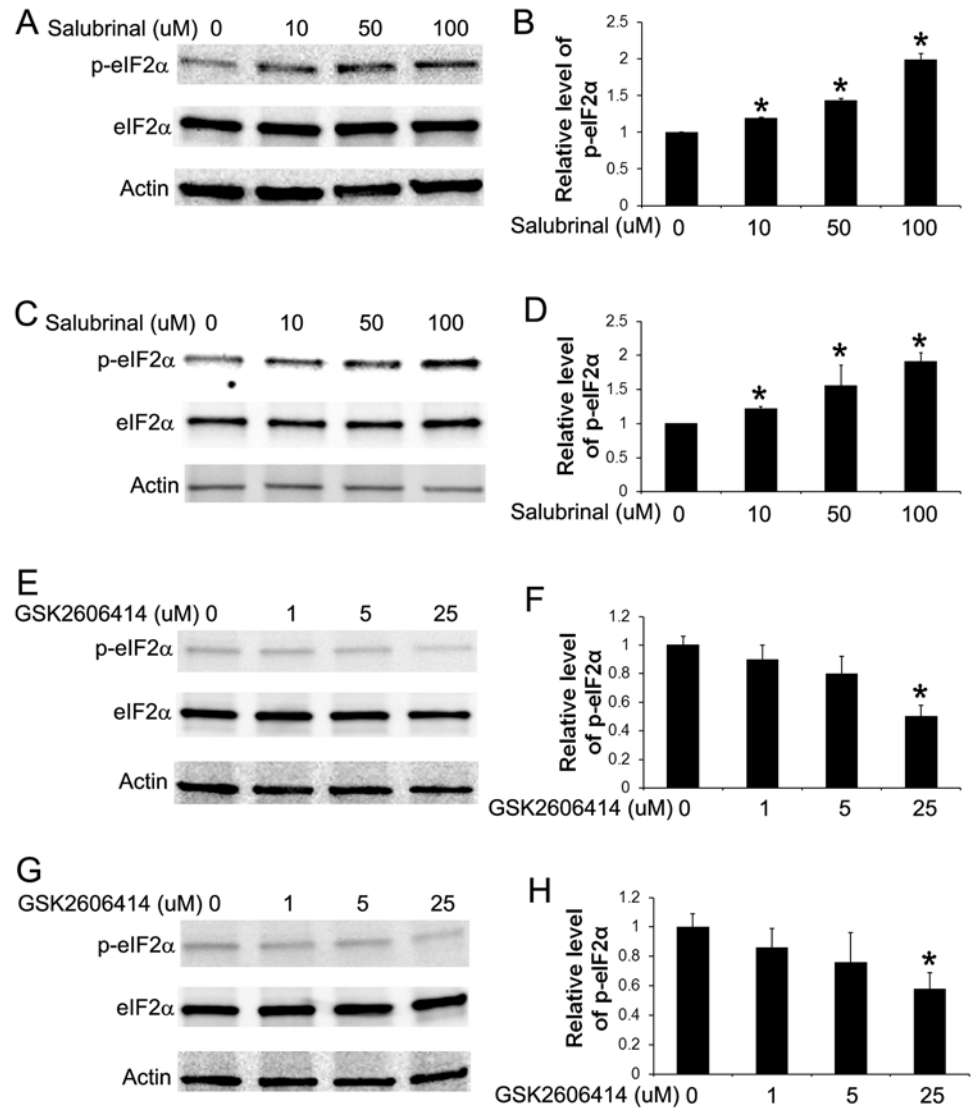**Fig 4. Treatment with either Salubrinal or GSK2606414 altered the levels of p-eIF2α in medulloblastoma cells.** (A, B) Western blot analysis showed that treatment with Salubrinal (10–100 μM) moderately but significantly elevated the level of p-eIF2α in Daoy cells. (C, D) Western blot analysis showed that treatment with Salubrinal (10–100 μM) moderately but significantly elevated the level of p-eIF2α in UW228 cells. (E, F) Western blot analysis showed that treatment with GSK2606414 (25 μM) noticeably decreased the level of p-eIF2α in Daoy cells. (G, H) Western blot analysis showed that treatment with GSK2606414 (25 μM) noticeably decreased the level of p-eIF2α in UW228 cells. The relative protein levels are relative to actin. The experiments were repeated at least three times. Error bars represent SD, $*P < 0.05$.

doi:10.1371/journal.pone.0120252.g004

[37, 38], or GSK2606414, a highly specific small molecule inhibitor of PERK kinase [39, 40]. Western blot analysis showed that treatment with Salubrinal (10–100 μM) moderately but significantly increased the level of p-eIF2α in both Daoy and UW228 cells (Fig. 4A, B, C, D). Real-time PCR analysis showed that Salubrinal treatment increased the expression of CHOP and GADD34 in both Daoy and UW228 cells, but did not significantly affect the expression of BIP (Fig. 3C, E). In contrast, treatment with GSK2606414 (25 μM) noticeably decreased the level of p-eIF2α in both Daoy and UW228 cells (Fig. 4E, F, G, H). Wound healing assay showed that treatment with the low dose of Salubrinal (10 μM) significantly facilitated Daoy and
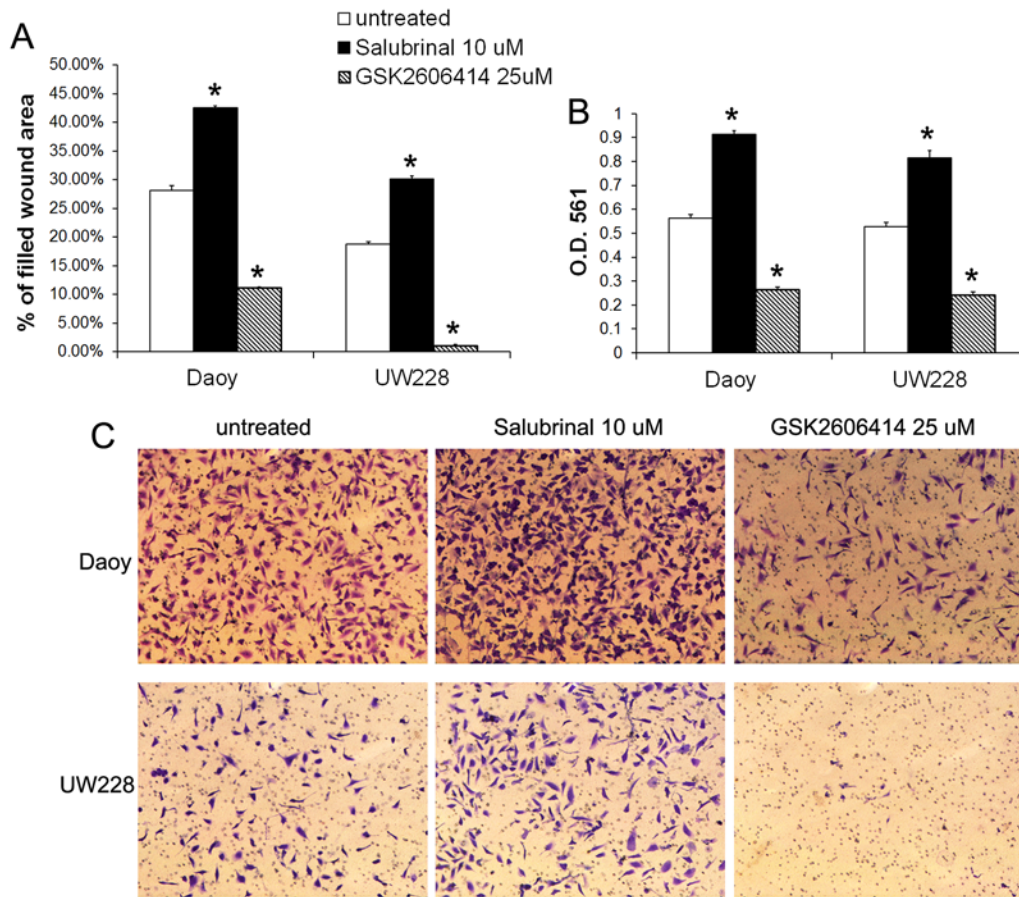
Fig 5. Moderate PERK activation enhanced medulloblastoma cell migration and invasion. (A) Wound healing assay showed that Salubrinal (10 µM) treatment significantly increased the percentage of filled wound area of Daoy and UW228 cells, and that GSK2606414 (25 µM) treatment significantly decreased the percentage of filled wound area of Daoy and UW228 cells. (B, C) Matrigel transwell assay showed that Salubrinal (10 µM) treatment significantly increased the numbers of the invaded Daoy and UW228 cells at the lower surface of the chamber, and that GSK2606414 (25 µM) treatment significantly decreased the numbers of the invaded Daoy and UW228 cells at the lower surface of the chamber. The experiments were repeated at least three times. Error bars represent SD, *$P < 0.05$.

UW228 cell migration, and that treatment with GSK2606414 (25 µM) significantly suppressed Daoy and UW228 cell migration (Fig. 5A). Matrigel transwell assay showed that 10 uM Salubrinal treatment significantly promoted the invasion of Daoy and UW228 cells, and that 25 µM GSK2606414 treatment significantly inhibited the invasion of Daoy and UW228 cells (Fig. 5B, C). Collectively, these data suggest that moderate activation of the PERK-eIF2α pathway promotes medulloblastoma cell migration and invasion.

Tumor cell-derived VEGF-A promotes medulloblastoma cell migration and invasion

A previous report has shown that medulloblastoma cells express VEGF-A and VEGFR2 and that treatment with a VEGFR2 inhibitor, SU5416, suppresses the cell growth [22]. Consistent with this report, we found that medulloblastoma cell lines, Daoy and UW228, expressed VEGF-A and VEGFR2 (Fig. 3), and that treatment with SU5416 (2.5–10 µM) significantly suppressed the growth of Daoy cells (Fig. 6A). Interestingly, wound healing assay showed that treatment with SU5416 (2.5–10 µM) resulted in a significant decrease in the migration capacity
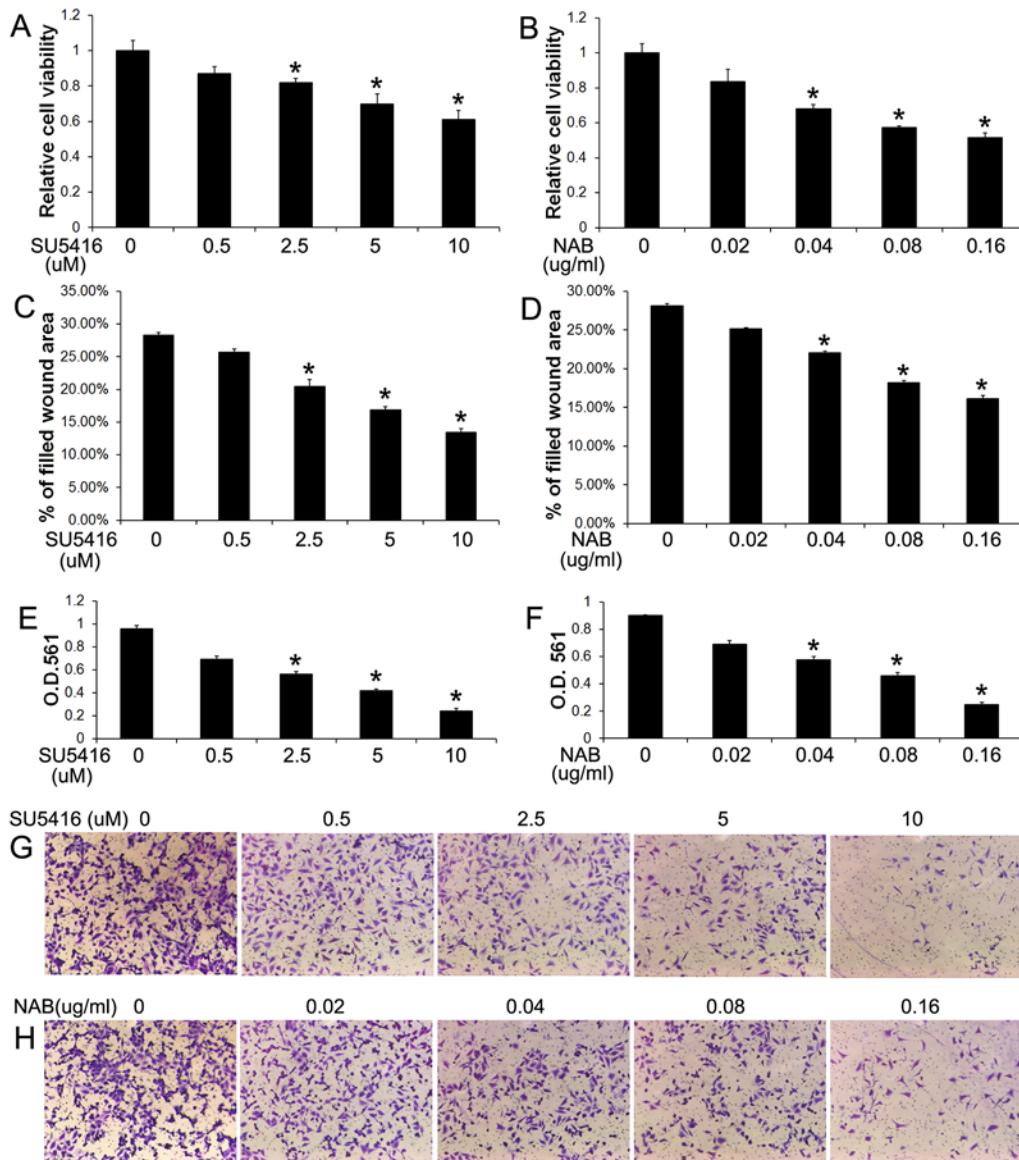
Fig 6. Blockage of VEGF-A impaired medulloblastoma cell migration and invasion. (A) MTT assay showed that SU5416 treatment significantly suppressed Daoy cell growth. (B) MTT assay showed that NAB treatment significantly suppressed Daoy cell growth. (C) Wound healing assay showed that SU5416 treatment significantly reduced the percentage of filled wound area of Daoy cells. (D) Wound-healing assay showed that NAB treatment significantly reduced the percentage of filled wound area of Daoy cells. (E, G) Matrigel transwell assay showed that SU5416 treatment significantly reduced the numbers of the invaded Daoy cells at the lower surface of the chamber. (F, H) Matrigel transwell assay showed that NAB treatment significantly reduced the numbers of the invaded Daoy cells at the lower surface of the chamber. The experiments were repeated at least three times. Error bars represent SD, *$P < 0.05$.

doi:10.1371/journal.pone.0120252.g006

of Daoy cells (Fig. 6C), as assessed by the percentage of filled wound area after 16 h of cell migration. Matrigel transwell assay showed that treatment with SU5416 (2.5–10 μM) led to a significant reduction in the invasion capacity of Daoy cells (Fig. 6E, G) and UW228 cells (Fig. 7D, E), as assessed by the number of cells that invaded through the matrigel. Thus, using the pharmacologic approach, our data suggest that VEGFR2 signaling is involved in medulloblastoma migration and invasion.

The activity of VEGFR2 can be regulated by a number of ligands, including VEGF-A [41]. To determine the autocrine role of VEGF-A in medulloblastoma migration and invasion, we
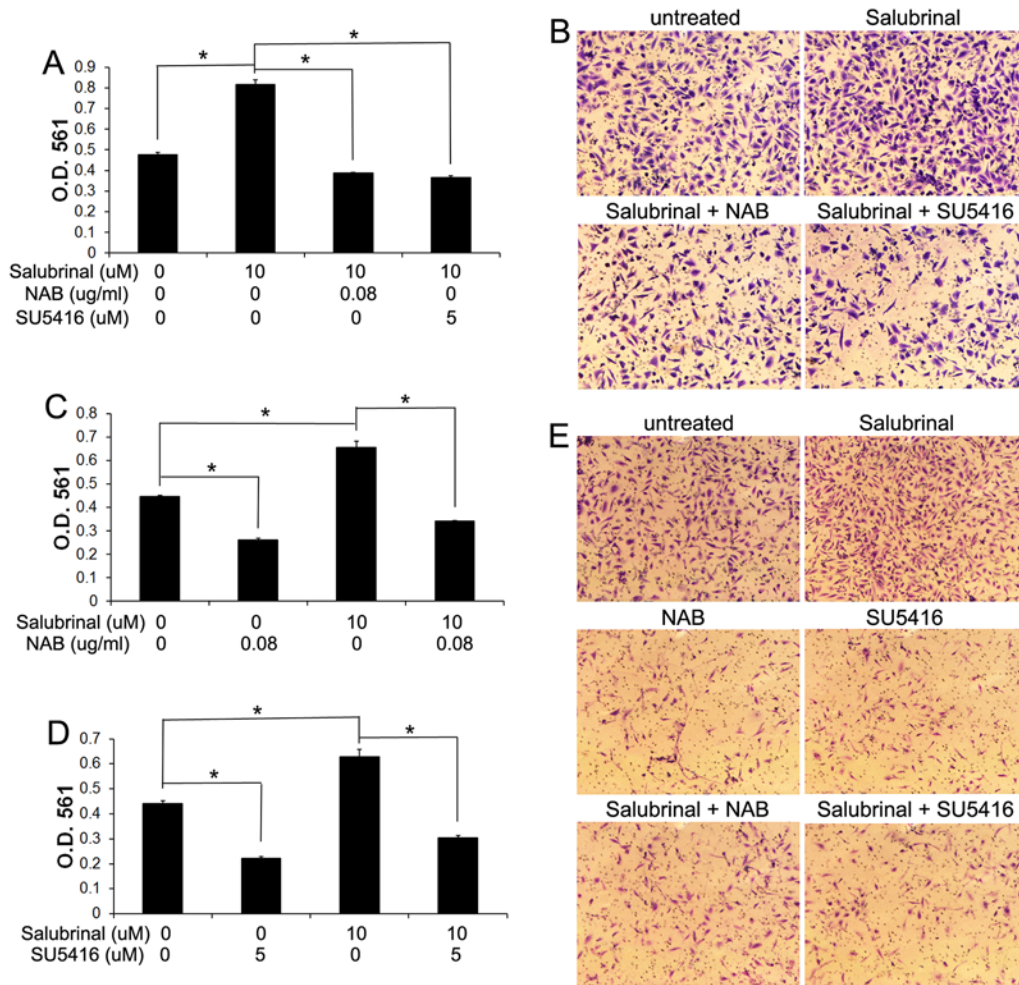
Fig 7. PERK activation promoted medulloblastoma cell invasion through activation of VEGF-A/VEGFR2 signaling. (A, B) Matrigel transwell assay showed that 10 μM Salubrinal treatment significantly increased the numbers of the invaded Daoy cells at the lower surface of the chamber. Interestingly, treatment with either 0.08 μg/ml NAB or 5 μM SU5416 diminished the increased cell number at the lower surface of the chamber induced by Salubrinal treatment. (C, E) Matrigel transwell assay showed that 10 μM Salubrinal treatment significantly increased the numbers of the invaded UW228 cells at the lower surface of the chamber; however, treatment with 0.08 μg/ml NAB significantly reduced the numbers of the invaded UW228 cells at the lower surface of the chamber. Interestingly, treatment with 0.08 μg/ml NAB also diminished the increased cell number at the lower surface of the chamber induced by Salubrinal treatment. (D, E) Matrigel transwell assay showed that treatment with 5 μM SU5416 significantly reduced the numbers of the invaded UW228 cells at the lower surface of the chamber. Importantly, 5 μM SU5416 treatment also diminished the increased cell number at the lower surface of the chamber induced by Salubrinal treatment. The experiments were repeated at least three times. Error bars represent SD, *$P < 0.05$.

doi:10.1371/journal.pone.0120252.g007

further exploited a VEGF-A neutralizing antibody (NAB). We found that treatment with the NAB (0.04–0.16 μg/ml) also significantly inhibited the growth of Daoy cells (Fig. 6B). Wound healing assay showed that treatment with the NAB (0.04–0.16 μg/ml) significantly reduced the migration capacity of Daoy cells (Fig. 6D). Furthermore, matrigel transwell assay showed that treatment with the NAB (0.04–0.16 μg/ml) significantly decreased the invasion capacity of Daoy cells (Fig. 6F, H) and UW228 cells (Fig. 7C, E). Thus, using the VEGFR2 inhibitor SU5416 and the NAB to block VEGF-A/VEGFR2 signaling, our data suggest that VEGF-A acts directly on medulloblastoma cells in an autocrine manner to promote cell migration and invasion.

VEGF-A is required for the promoting effects of moderate PERK activation on medulloblastoma cell migration and invasion

Several studies have shown that PERK activation increased VEGF-A expression in medulloblastoma cells [18, 23, 24]. We determined the involvement of VEGF-A in the promoting effects of PERK activation on medulloblastoma cell migration and invasion. As expected, real-time PCR analysis showed that 0.01 nM AP20187 treatment significantly elevated the mRNA levels of CHOP, GADD34, and VEGF-A, in Fv2E-PERK1 cells, but did not significantly affect the expression of VEGFR2 (Fig. 3A). ELISA measurement of VEGF-A production in culture supernatants showed that 0.01 nM AP20187 treatment stimulated Fv2E-PERK1 cells to secrete VEGF-A (Fig. 3B). Similarly, we found that 10 µM Salubrinal treatment resulted in the significant elevated mRNA levels of CHOP, GADD34, and VEGF-A in Daoy and UW228 cells, but had no effects on the VEGFR2 mRNA level (Fig. 3C, E). Moreover, ELISA measurement of VEGF-A production in culture supernatants revealed that 10 µM Salubrinal treatment significantly enhanced the secretion of VEGF-A in both Daoy and UW228 cells (Fig. 3D, F).

Wound healing assay showed that 0.01 nM AP20187 treatment significantly promoted Fv2E-PERK1 cell migration; however, 0.08 µg/ml NAB treatment diminished the ability of AP20187 treatment to promote cell migration (Fig. 8A). Matrigel transwell assay showed that 0.01 nM AP20187 treatment significantly increased the invaded Fv2E-PERK1 cell numbers at the lower surface of the chamber, and that 0.08 µg/ml NAB abrogated the increased number of invaded cells induced by AP20187 treatment (Fig. 8B, C). Moreover, matrigel transwell assay showed that 10 µM Salubrinal treatment significantly increased the invaded cell numbers of Daoy and UW228 at the lower surface of the chamber, and that 0.08 µg/ml NAB treatment impaired the ability of Salubrinal treatment to increase the number of invaded cells (Fig. 7A, B, C, E). Collectively, these data suggest that moderate PERK activation promotes medulloblastoma cell migration and invasion through induction of VEGF-A.

Furthermore, using the VEGFR2 inhibitor SU5416, our data suggested that VEGFR2 was required for the promoting effects of PERK activation on medulloblastoma cell migration and invasion. We found that the ability of 0.01 nM AP20187 treatment to promote Fv2E-PERK1 cell migration and invasion was diminished by treatment with 5 µM SU5416, as shown by wound-healing assay and matrigel transwell assay (Fig. 8), respectively. Additionally, matrigel transwell assay showed that 5 µM SU5416 treatment diminished the ability of 10 µM Salubrinal treatment to promote Daoy and UW228 cell invasion (Fig. 7). Thus, using the VEGFR2 inhibitor SU5416 and the NAB to block VEGF-A/VEGFR2 signaling, our results suggest that moderate PERK activation promotes medulloblastoma cell migration and invasion through activation of VEGF-A/VEGFR2 signaling.

Discussion

It is well documented that the PERK branch of the UPR is activated in solid tumors [5, 6, 9]. Recent reports suggest that activation of PERK signaling contributes to the promoting effects of hypoxia on breast cancer cell migration and invasion [12, 42]. In this study, our findings provided evidence that moderate activation of the PERK-eIF2α pathway enhanced medulloblastoma cell migration and invasion through activation of VEGF-A/VEGFR2 signaling. We found that moderately enhanced PERK activation, via a genetic approach or a pharmacologic approach, facilitated medulloblastoma cell migration and invasion and increased the production of VEGF-A. Moreover, using the VEGFR2 inhibitor SU5416 and the NAB to block VEGF-A/VEGFR2 signaling, our results suggested that both VEGF-A and its receptor VEGFR2 were required for the promoting effects of PERK activation on medulloblastoma cell migration and invasion.
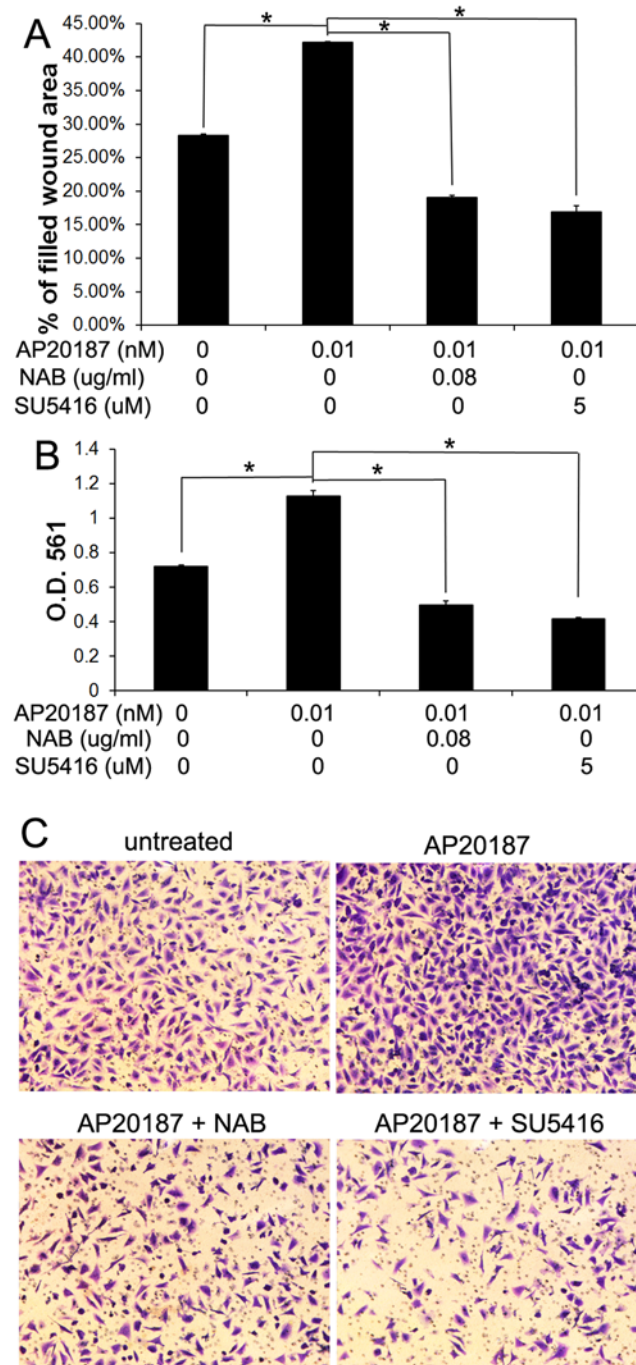
Fig 8. VEGF-A contributed to the promoting effects of PERK activation on Daoy cell migration and invasion. (A) Wound-healing assay showed that 0.01 nM AP20187 treatment significantly increased the percentage of filled wound area of Fv2E-PERK1 cells. Importantly, the increased percentage of filled wound area induced by AP20187 treatment was diminished by treatment with either 0.08 μg/ml NAB or 5 μM SU5416. (B, C) Matrigel transwell assay showed that 0.01 nM AP20187 treatment significantly increased the numbers of the invaded Fv2E-PERK1 cells at the lower surface of the chamber. Interestingly, treatment with either 0.08 μg/ml NAB or 5 μM SU5416 diminished the increased cell number at the lower surface of the chamber induced by AP20187 treatment. The experiments were repeated at least three times. Error bars represent SD, *$P < 0.05$.

doi:10.1371/journal.pone.0120252.g008

It is believed that PERK activation has biphasic effects on cell viability, dependent on the degree of activation [2, 43, 44]. Strong PERK activation in response to severe ER stress is detrimental to cells through inhibition of global protein translation and/or induction of CHOP, a pro-apoptotic transcription factor [8, 13, 31]. In contrast, moderate PERK activation adapts cells to mild ER stress under physiological and pathological conditions [8, 29, 30]. Herein, we used a genetic tool to generate stably transfected medulloblastoma cell lines that allow for dose-dependent activation of PERK by the small chemical compound AP20187, in the absence of ER stress. We showed that strong PERK activation induced by the high dose of AP20187 treatment severely inhibited protein translation in the medulloblastoma cells and suppressed cell growth. Not surprisingly, we also found that strong PERK activation suppressed the medulloblastoma cell migration and invasion (unpublished data). In contrast, moderately enhanced PERK activation induced by the low dose of AP20187 treatment slightly reduced protein translation in the medulloblastoma cells and had no significant effect on cell growth. Interestingly, moderately enhanced PERK activation promoted the medulloblastoma cell migration and invasion. Moreover, we found that moderately enhanced PERK activation induced by Salubrinal treatment enhanced medulloblastoma cell migration and invasion and that impaired PERK activation induced by GSK2606414 treatment suppressed medulloblastoma cell migration and invasion. Taken together, our data suggest that the effects of PERK activation on tumor cell migration and invasion are also dependent on the degree of activation, namely that moderate PERK activation is promoting, whereas strong PERK activation is suppressing.

VEGF-A is thought to play a critical role in tumor progression through enhancing angiogenesis [19]. Angiogenesis not only enhances tumor growth by supplying more nutrients and oxygen to the tumors, but also increases the opportunity for tumor cells to enter the circulation and disseminate. Moreover, there is evidence that VEGF-A can act directly on some tumor cell types in an autocrine manner to promote tumor growth and invasion [20, 21]. A number of studies reveal the elevated levels of VEGF-A and VEGFR2 in medulloblastoma of human patients [45, 46]. Recent studies also show that medulloblastoma cells express both VEGF-A and VEGFR2 [22, 47]. Nevertheless, the role of VEGF-A that plays in medulloblastoma remains elusive. A study reported that VEGF-A promotes medulloblastoma cell growth via VEGFR2 signaling [22]. Other studies, however, showed that VEGF-A has no effect on medulloblastoma cell migration and invasion [47, 48]. Using two medulloblastoma cell lines, Daoy and UW228, we demonstrated that these cell lines expressed both VEGF-A and VEGFR2. To determine the effects of VEGF-A/VEGFR2 signaling on medulloblastoma, we selected the well-documented VEGFR2 inhibitor SU5416 [22, 49] and the well-documented NAB [50, 51] to manipulate the activity of this pathway in medulloblastoma cells. As expected, we showed that treatment with either the NAB or the VEGFR2 inhibitor suppressed medulloblastoma cell growth when the cells were incubated in DMEM with 10% FBS. We also found that treatment with either the NAB or the VEGFR2 inhibitor had no significant effects on medulloblastoma cell viability under serum starvation conditions (unpublished data). Importantly, we showed that treatment with either the NAB or the VEGFR2 inhibitor suppressed medulloblastoma cell migration and invasion under serum starvation conditions. Therefore, these results suggest that VEGF-A acts directly on medulloblastoma cells in an autocrine manner to promote tumor migration and invasion. Unfortunately, we could not provide direct evidence for the autocrine role of VEGF-A/VEGFR2 signaling in medulloblastoma cells using a genetic approach, namely the RNA interference approach. Despite considerable efforts, we were not capable of establishing medulloblastoma cell lines that were stably transfected with VEGFR2 short hairpin RNA (shRNA). The possibilities that account for the contradictory results regarding the effects of VEGF-A on medulloblastoma cells could include the following: 1. different cell lines were used, Akino et al. [48] showed that VEGF-A did not affect D283, D425, D458 and D556 cell migration and

invasion because these cell lines do not express VEGFR2; 2. different experimental approaches were used, Davare et al. [47] showed that VEGF-A did not influence Daoy cell invasion because VEGF-A was added to the culture media in the lower chamber as chemoattractant.

After tumor cells accumulate mutations that overcome cell cycle and apoptotic checkpoints, they must acquire the abilities to adapt to the tumor microenvironment, to invade, and to promote angiogenesis, which is thought to be the critical step in tumor progression [52, 53]. Nevertheless, little is known about how medulloblastoma cells acquire these abilities. It is well documented that activation of the PERK branch of the UPR adapts tumor cells to the tumor microenvironment [10, 54, 55]. We showed here that moderately enhanced PERK activation promoted medulloblastoma cell migration and invasion, and increased the expression of VEGF-A, a master regulator of angiogenesis. Importantly, using the VEGFR2 inhibitor SU5416 and the NAB to block VEGF-A/VEGFR2 signaling, our results suggested that VEGF-A was required for the promoting effects of PERK activation on medulloblastoma cell migration and invasion. Taken together, these data imply that moderate PERK activation contributes to the abilities of medulloblastoma cells to adapt to the tumor microenvironment, to invade, and to promote angiogenesis. Furthermore, the results presented in this study indicate the role of VEGF-A in the promoting effects of moderate PERK activation on medulloblastoma invasion and angiogenesis.

Acknowledgments

Author Contributions

Conceived and designed the experiments: WL. Performed the experiments: SJ YL WL. Analyzed the data: SJ YL WL. Wrote the paper: SJ YL WL.

References

1. Marciniak SJ, Ron D. Endoplasmic reticulum stress signaling in disease. Physiol Rev. 2006; 86: 1133–1149. PMID: 17015486

2. Walter P, Ron D. The unfolded protein response: from stress pathway to homeostatic regulation. Science. 2011; 334: 1081–1086. doi: 10.1126/science.1209038 PMID: 22116877

3. Pavitt GD, Ron D. New insights into translational regulation in the endoplasmic reticulum unfolded protein response. Cold Spring Harb Perspect Biol. 2012; 4: a012278. doi: 10.1101/cshperspect.a012278 PMID: 22535228

4. Ron D, Walter P. Signal integration in the endoplasmic reticulum unfolded protein response. Nat Rev Mol Cell Biol. 2007; 8: 519–529. PMID: 17565364

5. Ma Y, Hendershot LM. The role of the unfolded protein response in tumour development: friend or foe? Nat Rev Cancer. 2004; 4: 966–977. PMID: 15573118

6. Moenner M, Pluquet O, Bouchecareilh M,.Chevet E. Integrated endoplasmic reticulum stress responses in cancer. Cancer Res. 2007; 67: 10631–10634. PMID: 18006802

7. Ackerman D, Simon MC. Hypoxia, lipids, and cancer: surviving the harsh tumor microenvironment. Trends Cell Biol. 2014; 24: 472–478. doi: 10.1016/j.tcb.2014.06.001 PMID: 24985940

8. Ranganathan AC, Ohja S, Kourtidis A, Conklin DS, Aguirre-Ghiso JA. Dual function of pancreatic endoplasmic reticulum kinase in tumor cell growth arrest and survival. Cancer Res. 2008; 68: 3260–3268. doi: 10.1158/0008-5472.CAN-07-6215 PMID: 18451152

9. Vandewynckel YP, Laukens D, Geerts A, Bogaerts E, Paridaens A, Verhelst X, et al. The paradox of the unfolded protein response in cancer. Anticancer Res. 2013; 33: 4683–4694. PMID: 24222102

10. Fels DR, Koumenis C. The PERK/eIF2alpha/ATF4 module of the UPR in hypoxia resistance and tumor growth. Cancer Biol Ther. 2006; 5: 723–728. PMID: 16861899

11. Atkins C, Liu Q, Minthorn E, Zhang SY, Figueroa DJ, Moss K, et al. Characterization of a novel PERK kinase inhibitor with antitumor and antiangiogenic activity. Cancer Res. 2013; 73: 1993–2002. doi: 10.1158/0008-5472.CAN-12-3109 PMID: 23333938

12. Mujcic H, Nagelkerke A, Rouschop KM, Chung S, Chaudary N, Span PN, et al. Hypoxic activation of the PERK/eIF2α arm of the unfolded protein response promotes metastasis through induction of LAMP3. Clin Cancer Res. 2013; 19: 6126–6137. doi: 10.1158/1078-0432.CCR-13-0526 PMID: 24045183

13. Lin JH, Li H, Zhang Y, Ron D, Walter P. Divergent effects of PERK and IRE1 signaling on cell viability. PLoS One. 2009; 4: e4170. doi: 10.1371/journal.pone.0004170 PMID: 19137072

14. Huber AL, Lebeau J, Guillaumot P, Pétrilli V, Malek M, Chilloux J, et al. p58(IPK)-mediated attenuation of the proapoptotic PERK-CHOP pathway allows malignant progression upon low glucose. Mol Cell. 2013; 28: 1049–1059.

15. Martín-Pérez R, Palacios C, Yerbes R, Cano-González A, Iglesias-Serret D, Gil J, et al. Activated ERBB2/HER2 licenses sensitivity to apoptosis upon endoplasmic reticulum stress through a PERK-dependent pathway. Cancer Res. 2014; 74: 1766–1777. doi: 10.1158/0008-5472.CAN-13-1747 PMID: 24453000

16. Crawford JR, MacDonald TJ, Packer RJ. Medulloblastoma in childhood: new biological advances. Lancet Neurol. 2007; 6: 1073–1085. PMID: 18031705

17. Northcott PA, Jones DT, Kool M, Robinson GW, Gilbertson RJ, Cho YJ, et al. Medulloblastomics: the end of the beginning. Nat Rev Cancer. 2012; 12: 818–834. doi: 10.1038/nrc3410 PMID: 23175120

18. Lin W, Lin Y, Li J, Harding HP, Ron D, Jamison S. A deregulated integrated stress response promotes interferon-γ-induced medulloblastoma. J Neurosci Res. 2011; 89: 1586–1595. doi: 10.1002/jnr.22693 PMID: 21688289

19. Hicklin DJ, Ellis LM. Role of the vascular endothelial growth factor pathway in tumor growth and angiogenesis. J Clin Oncol. 2005; 23: 1011–1027. PMID: 15585754

20. Mercurio AM, Bachelder RE, Bates RC, Chung J. Autocrine signaling in carcinoma: VEGF and the alpha6beta4 integrin. Semin Cancer Biol. 2004; 14: 115–122. PMID: 15018895

21. Lichtenberger BM, Tan PK, Niederleithner H, Ferrara N, Petzelbauer P, Sibilia M. Autocrine VEGF signaling synergizes with EGFR in tumor cells to promote epithelial cancer development. Cell. 2010; 140: 268–279. doi: 10.1016/j.cell.2009.12.046 PMID: 20141840

22. Slongo ML, Molena B, Brunati AM, Frasson M, Gardiman M, Carli M, et al. Functional VEGF and VEGF receptors are expressed in human medulloblastomas. Neuro Oncol. 2007; 9: 384–392. PMID: 17704359

23. Pereira ER, Liao N, Neale GA, Hendershot LM. Transcriptional and post-transcriptional regulation of proangiogenic factors by the unfolded protein response. PLoS One. 2010; 5: e12521. doi: 10.1371/journal.pone.0012521 PMID: 20824063

24. Pereira ER, Frudd K, Awad W, Hendershot LM. Endoplasmic reticulum (ER) stress and hypoxia response pathways interact to potentiate hypoxia-inducible factor 1 (HIF-1) transcriptional activity on targets like vascular endothelial growth factor (VEGF). J Biol Chem. 2014; 289: 3352–3364. doi: 10.1074/jbc.M113.507194 PMID: 24347168

25. Keles GE, Berger MS, Srinivasan J, Kolstoe DD, Bobola MS, Silber JR. Establishment and characterization of four human medulloblastoma-derived cell lines. Oncol Res. 1995; 7: 493–503. PMID: 8866661

26. Lu PD, Jousse C, Marciniak SJ, Zhang Y, Novoa I, Scheuner D, et al. Cytoprotection by pre-emptive conditional phosphorylation of translation initiation factor 2. EMBO J. 2004; 23: 169–179. PMID: 14713949

27. Lin W, Harding HP, Ron D, Popko B. Endoplasmic reticulum stress modulates the response of myelinating oligodendrocytes to the immune cytokine interferon-gamma. J Cell Biol. 2005; 169: 603–612. PMID: 15911877

28. Lin Y, Jamison S, Lin W. Interferon-γ activates nuclear factor-κ B in oligodendrocytes through a process mediated by the unfolded protein response. PLoS One. 2012; 7: e36408. doi: 10.1371/journal.pone.0036408 PMID: 22574154

29. Lin W, Lin Y, Li J, Fenstermaker AG, Way SW, Clayton B, et al. Oligodendrocyte-specific activation of PERK signaling protects mice against experimental autoimmune encephalomyelitis. J Neurosci. 2013; 33: 5980–5991. doi: 10.1523/JNEUROSCI.1636-12.2013 PMID: 23554479

30. Lin Y, Huang G, Jamison S, Li J, Harding HP, Ron D, et al. PERK activation preserves the viability and function of remyelinating oligodendrocytes in immune-mediated demyelinating diseases. Am J Pathol. 2014; 184: 507–519. doi: 10.1016/j.ajpath.2013.10.009 PMID: 24269558

31. Lin Y, Pang X, Huang G, Jamison S, Fang J, Harding HP, et al. Impaired eukaryotic translation initiation factor 2B activity specifically in oligodendrocytes reproduces the pathology of Vanishing White Matter

Disease in mice. J Neurosci. 2014; 34: 12182–12191. doi: 10.1523/JNEUROSCI.1373-14.2014 PMID: 25186761

32. Lin W, Lin Y. Interferon-γ inhibits central nervous system myelination through both STAT1-dependent and STAT1-independent pathways. J Neurosci Res. 2010; 88:2569–2577. doi: 10.1002/jnr.22425 PMID: 20648647

33. Schmidt EK, Clavarino G, Ceppi M, Pierre P. SUnSET, a nonradioactive method to monitor protein synthesis. Nat Methods. 2009; 6: 275–277. doi: 10.1038/nmeth.1314 PMID: 19305406

34. Harding HP, Zhang Y, Ron D. Protein translation and folding are coupled by an endoplasmic-reticulum-resident kinase. Nature. 1999; 397: 271–274. PMID: 9930704

35. Harding HP, Novoa I, Zhang Y, Zeng H, Wek R, Schapira M, et al. Regulated translation initiation controls stress-induced gene expression in mammalian cells. Mol Cell. 2000; 6:1099–1108. PMID: 11106749

36. Qi L, Yang L, Chen H. Detecting and quantitating physiological endoplasmic reticulum stress. Methods Enzymol. 2011; 490: 137–146. doi: 10.1016/B978-0-12-385114-7.00008-8 PMID: 21266248

37. Boyce M, Bryant KF, Jousse C, Long K, Harding HP, Scheuner D, et al. A selective inhibitor of eIF2alpha dephosphorylation protects cells from ER stress. Science. 2005; 307: 935–939. PMID: 15705855

38. Lin W, Kunkler PE, Harding HP, Ron D, Kraig RP, Popko B. Enhanced integrated stress response promotes myelinating oligodendrocyte survival in response to interferon-gamma. Am J Pathol., 2008; 173: 1508–1517. doi: 10.2353/ajpath.2008.080449 PMID: 18818381

39. Axten JM, Medina JR, Feng Y, Shu A, Romeril SP, Grant SW, et al. Discovery of 7-methyl-5-(1-{[3-(trifluoromethyl)phenyl]acetyl}-2,3-dihydro-1H-indol-5-yl)-7H-pyrrolo[2,3-d]pyrimidin-4-amine (GSK2606414), a potent and selective first-in-class inhibitor of protein kinase R (PKR)-like endoplasmic reticulum kinase (PERK). J Med Chem. 2012; 55: 7193–7207. doi: 10.1021/jm300713s PMID: 22827572

40. Harding HP, Zyryanova AF, Ron D. Uncoupling proteostasis and development in vitro with a small molecule inhibitor of the pancreatic endoplasmic reticulum kinase, PERK. J Biol Chem. 2012; 287: 44338–44344. doi: 10.1074/jbc.M112.428987 PMID: 23148209

41. Carmeliet P, Ruiz de Almodovar C. VEGF ligands and receptors: implications in neurodevelopment and neurodegeneration. Cell Mol Life Sci. 2013; 70: 1763–1778. doi: 10.1007/s00018-013-1283-7 PMID: 23475071

42. Nagelkerke A, Bussink J, Mujcic H, Wouters BG, Lehmann S, Sweep FC, et al. Hypoxia stimulates migration of breast cancer cells via the PERK/ATF4/LAMP3-arm of the unfolded protein response. Breast Cancer Res. 2013; 15: R2. doi: 10.1186/bcr3373 PMID: 23294542

43. Tabas I, Ron D. Integrating the mechanisms of apoptosis induced by endoplasmic reticulum stress. Nat Cell Biol. 2011; 13: 184–190. doi: 10.1038/ncb0311-184 PMID: 21364565

44. Hetz C. The unfolded protein response: controlling cell fate decisions under ER stress and beyond. Nat Rev Mol Cell Biol. 2012; 13: 89–102. doi: 10.1038/nrm3270 PMID: 22251901

45. Smith ER, Zurakowski D, Saad A, Scott RM, Moses MA. Urinary biomarkers predict brain tumor presence and response to therapy. Clin Cancer Res. 2008; 14: 2378–2386. doi: 10.1158/1078-0432.CCR-07-1253 PMID: 18413828

46. Hervey-Jumper SL, Garton HJ, Lau D, Altshuler D, Quint DJ, Robertson PL, et al. Differences in vascular endothelial growth factor receptor expression and correlation with the degree of enhancement in medulloblastoma. J Neurosurg Pediatr. 2014; 14: 121–128. doi: 10.3171/2014.4.PEDS13244 PMID: 24905841

47. Davare MA, Lal S, Peckham JL, Prajapati SI, Gultekin SH, Rubin BP, et al. Secreted meningeal chemokines, but not VEGFA, modulate the migratory properties of medulloblastoma cells. Biochem Biophys Res Commun. 2014; 450: 555–560. doi: 10.1016/j.bbrc.2014.06.018 PMID: 24928387

48. Akino T, Han X, Nakayama H, McNeish B, Zurakowski D, Mammoto A, et al. Netrin-1 promotes medulloblastoma cell invasiveness and angiogenesis, and demonstrates elevated expression in tumor tissue and urine of patients with pediatric medulloblastoma. Cancer Res. 2014; 74: 3716–3726. doi: 10.1158/0008-5472.CAN-13-3116 PMID: 24812271

49. Mendel DB, Laird AD, Smolich BD, Blake RA, Liang C, Hannah AL, et al. Development of SU5416, a selective small molecule inhibitor of VEGF receptor tyrosine kinase activity, as an anti-angiogenesis agent. Anticancer Drug Des. 2000; 15:29–41. PMID: 10888034

50. Hashizume H, Falcón BL, Kuroda T, Baluk P, Coxon A, Yu D, et al. Complementary actions of inhibitors of angiopoietin-2 and VEGF on tumor angiogenesis and growth. Cancer Res. 2010; 70:2213–2223. doi: 10.1158/0008-5472.CAN-09-1977 PMID: 20197469

51. Moreira IS, Fernandes PA, Ramos MJ. Vascular endothelial growth factor (VEGF) inhibition—a critical review. Anticancer Agents Med Chem. 2007; 7:223–245. PMID: 17348829

52. Hanahan D, Weinberg RA. The hallmarks of cancer. Cell. 2000; 100: 57–70. PMID: 10647931

53. Hanahan D, Weinberg RA. Hallmarks of cancer: the next generation. Cell. 2011; 144: 646–674. doi: 10.1016/j.cell.2011.02.013 PMID: 21376230

54. Bi M, Naczki C, Koritzinsky M, Fels D, Blais J, Hu N, et al. ER stress-regulated translation increases tolerance to extreme hypoxia and promotes tumor growth. EMBO J. 2005; 24: 3470–3481. PMID: 16148948

55. Rouschop KM, van den Beucken T, Dubois L, Niessen H, Bussink J, Savelkouls K, et al. The unfolded protein response protects human tumor cells during hypoxia through regulation of the autophagy genes MAP1LC3B and ATG5. J Clin Invest. 2010; 120: 127–141. doi: 10.1172/JCI40027 PMID: 20038797